Effect of Travoprost, Latanoprost and Bimatoprost PGF2α Treatments on the biomechanical properties of in-vivo rabbit cornea

JunJie Wang [1,2], YiPing Zhao [3], AYong Yu [1], Jie Wu [1], ManMan Zhu [1], MuChen Jiang [1], DaTian Zhu [1], PeiPei Zhang [1], XiaoBo Zheng [1,2 *], FangJun Bao [1,2*], Ahmed Elsheikh [4,5,6]

JunJie Wang, YiPing Zhao, AYong Yu are co-first authors of the article.

[1] Eye Hospital, Wenzhou Medical University, Wenzhou 325027, China

[2] The Institution of Ocular Biomechanics, Wenzhou Medical University, Wenzhou 325027, China

[3] Department of Ophthalmology, Ninth People's Hospital, Shanghai JiaoTong University School of Medicine, No.639 ZhizaojuRoad, Shanghai, 200025, China

[4] School of Engineering, University of Liverpool, Liverpool L69 3GH, UK

[5] National Institute for Health Research (NIHR) Biomedical Research Centre for Ophthalmology, Moorfields Eye Hospital NHS Foundation Trust and UCL Institute of Ophthalmology, London, UK

[6] Beijing Advanced Innovation Center for Biomedical Engineering, Beihang University, Beijing, China

Abbreviated title:

Influence of 3 kinds of PGF2α on corneal biomechanical properties

Acknowledgement

The authors thank Dr Shen LJ of WenZhou Medical University for the technical assistance he provided for this study.

Financial Support:

This study was supported by the Zhejiang Provincial Natural Science Foundation of China under Grant (LY20H120001, LY18A020008, LQ20A020008), the National Natural Science Foundation of China (31771020, 82001924), the Projects of Medical and Health Technology Development Program in Zhejiang Province (2019RC056, 2018KY541, 2016ZHB012), Science and Technology Plan Project of Wenzhou Science and Technology Bureau (Y2020354, Y20180172, Y20170198, Y20170792) and the General Projects of Department of Education of Zhejiang Province (Y201839651).

Co-Corresponding author

Mr. XiaoBo Zheng

No. 270 Xueyuan West Road, WenZhou City, ZheJiang Prov, 325027, China

e-mail: xbjay911@126.com

Tel: 86-577-88067937; Fax: 86-577-88824115

Corresponding author

Dr. FangJun Bao

No. 270 XueYuan West Road, WenZhou City, ZheJiang Prov, 325027, China

e-mail: bfjmd@126.com

Tel: 86-571-88193999; Fax: 86-571- 86795926

Abstract:

Prostaglandin F2α analogues (PGF2α), one of the most commonly prescribed classes of hypotensive agents, could decrease collagen fibril density and remodel the extracellular matrix in cornea. We hypothesized that PGF2α's would induce corneal softening, reduce the accuracy of intraocular pressure (IOP) measurement and lead to uncertainty in the effectiveness of the therapy. We determined the stress-strain behavior of rabbit cornea after PGF2α usage and evaluated the effect of biomechanical changes associated with PGF2α treatment on IOP measurements by Goldmann Applanation Tonometry (GAT). The tangent modulus and fibril diameter decreased after PGF2α treatment, while the stromal interfibrillar spacing increased. PGF2α was shown to also affect the lateral eye with lower effect, which did not undergo direct eyedrop treatment. Significant decreases in the numerical predictions of GAT-IOP were predicted in all treated groups relative to control groups. Different PGF2α's (travoprost, latanoprost and bimatoprost) were associated with different extents of reduction in tissue stiffness and changes in corneal microstructure. These effects were only statistically significant in travoprost. PGF2α-induced changes in corneal mechanical properties could reduce the accuracy of IOP measurement and may cause an overestimation of the effect of PGF2α in lowering IOP, possibly leading to uncertainties in glaucoma management.

Keywords: prostaglandin; cornea; biomechanics

1. Introduction

Prostaglandin analogues (PGA), one of the most commonly prescribed classes of topical hypotensive agents, are frequently used as a first-line monotherapy for patients with primary open angle glaucoma (POAG) or ocular hypertension (OHT) (Li et al., 2016). Prostaglandin F2α analogues (PGF2α) reduce IOP by enhancing the aqueous humour outflow through the uveoscleral pathway to the suprachoroidal space and the episcleral veins (Gabelt and Kaufman, 1989; Lee et al., 1984). This outcome is achieved through upregulation of the activity of matrix metalloproteinases (MMP) and downregulation of the inhibitors of MMPs (TIMP) (Lindsey et al., 1996; Schachtschabel et al., 2000; Weinreb et al., 2004), both of which decrease collagen fibril density and remodel the extracellular matrix in the ciliary body, the sclera (Sagara et al., 1999; Tamm et al., 1990) and the cornea (Lopilly Park et al., 2012), which probably lead to changes in biomechanical properties.

Corneal stiffness, or biomechanical resistance to deformation under internal or external forces, is mainly determined by the tissue's microstructure and the biomechanics of its underlying components including the fibroblasts and extracellular matrix. Our earlier study reported significant reductions in corneal material stiffness associated with the use of travoprost – a form of PGF2α (Zheng et al., 2019). The mechanism leading to these reductions was believed to be related to a remodeling of corneal microstructure. Other reports noted significant changes in corneal thickness with PGF2α topical therapy, possibly due to the activation of MMPs (Schlote et al., 2009; Zhong et al., 2011). The combined effect of PGF2α in remodeling the microstructure and reducing corneal thickness would therefore be expected to lead to a stiffness loss and could be behind the increased risk of keratoconus progression, myopic regression and post-refractive surgery ectasia development as noted in earlier studies (Amano et al., 2008; Kamiya et al., 2008).

Within the context of glaucoma, the use of PGF2α presents a challenging question. While the therapy has been successful in lowering the intraocular pressure (IOP) – the main modifiable risk factor for glaucoma progression(Jonas et al., 2017) – the long term use of PGF2α may lead

to corneal stiffness reduction and hence underestimation in IOP measurements. In this study, we propose a hypothesis that PGF2α-induced corneal softening would reduce the accuracy of IOP measurement and could lead to uncertainty in the effectiveness of the therapy and whether the reduction observed in IOP measurement is due partly to the PGF2α's effect on corneal biomechanics. Considering the importance of corneal biomechanical behavior in the measurement of IOP (Bao et al., 2016; Liu and Roberts, 2005), this study was undertaken to evaluate the effect on the corneal material properties and microstructure of three commonly used forms of PGF2α, namely travoprost and latanoprost (both ester prodrug of PGF2α), and bimatoprost (amide prodrug of 17-phenyl-PGF2α). The study further sought to quantify the influence of the changes in corneal biomechanics on the IOP measurements made by the Goldmann Applanation Tonometer (GAT), the reference standard in tonometry.

2. Materials and methods

2.1. Experimental animals

The study was approved by the Animal Care and Ethics Committee of the University's Eye Hospital and all animals were treated in agreement with the ARVO Statement for Use of Animals in Ophthalmic and Vision Research. 96 Japanese white rabbits (obtained from the Animal Breeding Unit of the Wenzhou Medical University) weighing between 2 and 3 kg were housed in individual cages where the temperature and humidity were well controlled, and each rabbit was fed a standard chow and water and kept with a 12 hour light/darkness cycle. Before the establishment of drug model, the rabbits were allowed to acclimatize for at least 1 week.

The rabbits were randomly assigned to 4 groups of 24 rabbits each, namely the travoprost group (TR), latanoprost group (LA), bimatoprost group (BI) and the blank control (BC) group. The left eyes of the first 3 groups were divided into 3 treated subgroups, named as TRT, LAT and BIT subgroups and treated with travoprost (0.04 mg/ml, Travatan, Alcon, Herts, UK), latanoprost (0.05 mg/ml, Xalatan, Pfizer, Puurs, Belgium) and bimatoprost (0.3 mg/ml, Lumigan, Allergan, Mayo, Ireland) eyedrops once daily for 12 weeks around 4:30 pm to 7:30 pm. The right eyes of the same 3 groups remained untreated and formed 3 control subgroups

named TRC, LAC and BIC, respectively. As it was possible for the untreated right eyes in these subgroups to be affected by the treatment delivered to the left eyes, a fourth blank control (BC) group was added to the study. This group included only the left eyes of the 24 rabbits included in line with the formation of the other control subgroups. 18 eyes of each of the 7 subgroups were inflated to determine their biomechanical properties, while the remaining 6 were tested for microstructure.

Central corneal thickness (CCT) as well as intraocular pressure (IOP) were monitored before (pre) and each week after drops usage (1 week: pos1w to 12 weeks: pos12w) throughout the duration of the study. After topical anaesthesia (single drop of 0.5% proparacaine), CCT and IOP were measured by a portable pachymeter (PachPen, Accutome Inc, PA, USA) and a Tono-pen tonometer (Reichert, Inc., New York, USA), respectively. For each eye, three measurements were made, and the results were averaged. All examinations were made by the same operator (YPZ) during the same hours (between 8 and 11 AM).

2.2. Experimental design

Twelve weeks following treatment with PGF2αdrops, the rabbits in all groups were sacrificed by an intravenous injection of pentobarbital sodium overdose (Merck, Darmstadt, Germany) of 100 mg/kg body weight and the bilateral eyes were immediately enucleated. The corneas of 18 eyes in each subgroup were separated along with a 3-mm wide ring of scleral tissue before mounting them onto a custom built pressure chamber filled with Phosphate Buffered Saline (PBS, Maixin, China) (Ni et al., 2011; Yu et al., 2013; Yu et al., 2014) and mechanical clamps were used to tightly connect the scleral ring with the chamber. The pressure inside the chamber was controlled by a syringe pump whose movement was in turn controlled by a custom-built LabView software.

An ultrasonic pachymeter (SP-3000, Tomey Inc, Nagoya, Japan) was used to take central and peripheral thickness measurements (the latter taken approximately 1.5 mm away from the limbus), and a Vernier caliper was utilized to measure corneal diameters in four directions (horizontal, vertical, and two 45º diagonal directions). Side images of the cornea were obtained

using 3 digital cameras (EOS 60D, Canon, Inc., Tokyo, Japan) pointed at the corneal apex with 120° between each two. The resulting images were analyzed using Image J software (National Institutes of Health, Bethesda, MD, USA) to obtain the anterior corneal shape, and the posterior corneal shape was subsequently determined using the thickness measurements.

2.3. Biomechanical Inflation Testing

The pressure chamber formed part of a cornea inflation test rig (Figure 1) described previously (Bao et al., 2017; Ni et al., 2011; Yu et al., 2013; Yu et al., 2014). An initial inflation pressure of 2.0 mmHg was set up for all specimens to ensure a fully inflated and wrinkle-free corneal surface at start of test. The displacement at corneal apex was monitored continually through a CCD laser displacement sensor (LK series, Keyence, Milton Keynes, UK), which was connected to a personal computer to record the data. To condition and stabilize the behavior, three cycles of loading and unloading up to a pressure of 30.0 mmHg were applied at a rate of 0.10 mmHg/s, which ensured repeatable corneal responses as reported previously (Zhu et al., 2020). A recovery period of 90 seconds was allowed between each two loading cycles to ensure the behavior was not affected by the strain history of loading cycles (Yu et al., 2014), (Zheng et al., 2016). Finally, the specimens were subjected to a fourth loading cycle up to 30.0 mmHg, the results of which were used in a subsequent inverse analysis. All specimens were tested within 3 hours postmortem.

2.4 Inverse Analysis

An inverse analysis process was conducted to evaluate the material properties of corneal tissue based on the experimental pressure-deformation results. As described in previous studies (Bao et al., 2017; Zheng et al., 2016), the finite element (FE) solver Abaqus (Dassault Systèmes Simulia Corp., Rhode Island, USA) and optimization software package LS-OPT (Livermore Software Technology Corp, CA, USA) were used to implement the iterative process of the inverse analysis process.

The inverse analysis relied on finite element models built for each cornea included in the study.

The models adopted the initial geometries of specimens including their anterior topography (obtained from initial camera images), thickness profile and diameter measurements. Each model consisted of 1728 15-noded continuum elements (C3D15H), arranged in twelve rings and two layers, Figure 1B. A fully restricted model edge was assumed at the limbus to simulate connection to the mechanical clamps. A first order hyperelastic Ogden model (Yu et al., 2013; Yu et al., 2014),(Mulhern et al., 2001) was used to represent corneal material behavior using a strain energy density function in the form:

$$W = \frac{2\mu}{a^2}\left(\overline{\lambda_1}^{\alpha} + \overline{\lambda_2}^{\alpha} + \overline{\lambda_3}^{\alpha} - 3\right) + \frac{1}{D}(J-1)^2 \quad (1)$$

where W represents the strain energy per unit volume, $\overline{\lambda_k}$ the deviatoric principal stretches = $J^{-1/3} \times \lambda_k$ (k=1, 2, 3), λ_1, λ_2, λ_3 the principal stretches, $J = \lambda_1\lambda_2\lambda_3$. Material parameters μ and α are the strain hardening exponent and shear modulus, respectively. D is a compressibility parameter $= \frac{3(1-2\nu)}{\mu(1+\nu)}$ calculated assuming corneal tissue was nearly incompressible (Grupcheva et al., 2001),(Dhaliwal et al., 2001) with a Poisson's ratio, ν, of 0.48 (Bao et al., 2017; Yu et al., 2013).

The inverse analysis was carried out to determine the material parameters μ and α for each cornea by searching for the best combination of the parameters that minimized the root mean square (*RMS*) of mismatch between the experimental and numerical displacements at corneal apex using the following objective function:

$$RMS = \sqrt{\frac{1}{P}.\sum_{p=1}^{P}(\delta_p^{exp} - \delta_p^{num})^2} \quad (2)$$

where P is the total number of pressure levels (i.e. 2, 4, … up to 30 mmHg), and δ_p^{exp} and δ_p^{num} represent the experimental and numerical displacements of the corneal apex at each pressure level p. This process was implemented in the LS-OPT software and the search ranges for μ and α were from 0.001 to 0.1, and from 50 to 250, respectively, which were wide enough in all analyses. The inverse process took 15 to 20 iterations to converge, corresponding to 150 to 200 simulations (10 simulations in each iteration). The feasibility and solution uniqueness of the inverse optimization using LS-OPT were accessed previously (Zhu et al., 2020).

2.5. Histological Analysis

Histological analysis of six corneas from each specimen group was carried out to quantify the collagen components and interfibrillar spacing. The corneas were fixed, embedded in paraffin, sectioned on the sagittal plane and stained with Masson's trichrome by an experienced pathologist (LLP). Three 50nm-thick sections were removed from each cornea at 80, 180 and 280 μm under the epithelium, representing the anterior, intermediate and posterior corneal stroma layers, respectively. These sections were analyzed with a H-7500 transmission electron microscope (Hitachi, Japan) with ×40,000 magnification. The mean diameter of fibrils (2*r) in a TEM image was calculated from the fibril's cross sections, while the interfibrillar spacing was determined using Image J as described in a previous study (Bao et al., 2017). Only fibrils with clearly defined circular borders and high contrast were considered. Fibril cross-sections with an elliptical form were discarded in fibril diameter calculations (Wollensak et al., 2004). On the other hand, the interfibrillar spacing (D) was calculated as:

$$\mathrm{D} = \sqrt{\mathrm{Area/number\ of\ fibrils}} - 2 \times \mathrm{r}. \quad (3)$$

The mean values of D and r obtained from five TEM images taken for each section were calculated and used in later analysis. The number of fibrils per unit area (μm^2) was calculated as $\frac{10^6}{\pi \times (\frac{D}{2}+r)^2}$, where *D* and *r* were in nm. The number of fibrils per unit area normalized by corneal stromal thickness (CST), in μm, was calculated as $\frac{CST \times 10^6}{(\pi \times (\frac{D}{2}+r)^2}$. Epithelium thickness (EPT) was taken as 40 μm, and endothelium thickness (ENT) was assumed to be 10 μm as indicated in a previous study (Zhang et al., 2015), while CST was calculated as CCT – EPT - ENT.

2.6 Numerical simulation of Goldmann tonometer measurements

To evaluate the effects of corneal biomechanical changes caused by the PGF2α treatment on tonometry, the specimen-specific numerical models used in the inverse analysis process were extended to simulate the whole eye globes and their behaviour under both IOP and the GAT pressure. In these models, the sclera was assumed to have a spherical external surface with a diameter of 21 mm adopted from published measurement (Mattson et al., 2010) and a uniform

thickness which was the same as the peripheral corneal thickness as implemented in an earlier simulation study (Sinha Roy and Dupps, 2011). The sclera was divided into three regions, namely the anterior, equatorial and posterior parts, whose material properties were set to be 2 times, 1.9 times and 1.8 times of the stiffness of the cornea, following published rabbit data (Xie et al., 2018). A narrow limbus region was used to connect the cornea and the anterior sclera, and the region was assigned the same material properties as the anterior sclera, an approach adopted from one of our earlier publications (Bao et al., 2018). The boundary conditions were set to constrain motions at equatorial nodes in the anterior-posterior direction and at the pole nodes (X=0 and Y=0) in superior-inferior and nasal-temporal directions. On the other hand, the Goldmann tonometer tip was modelled as an undeformable rigid body with 54 R3D3 elements and 3.06 mm diameter. Three IOP levels, namely 10, 20 and 30 mmHg, that cover the normal physiological range and cases with ocular hypertension were considered in the study.

After inflating the globe model with IOP, a central force was applied on the tonometer tip and gradually increased until the cornea was applanated over the full 3.06 mm diameter. This applanation force, F, was then used to provide an IOP estimate while considering the surface tension effect of the tear film, GAT-IOP = F/A - T, where $A = (3.06)^2 \bullet \pi/4$ mm^2 was the tonometer tip area (Figure 2) and T = 0.000059 N/mm^2 was the equivalent pressure caused by tear film surface tension (Elsheikh et al., 2006).

2.7 Statistical analysis

All analyses were performed using the SPSS Statistics 20.0 (SPSS Inc., Chicago, USA). According to the results of a normal distribution test, comparisons between treated and lateral control specimen groups were performed using either the paired t-test or the Wilcoxon test, while One-way analysis of variance (ANOVA) or the Kruskal-Wallis H test was carried out to compare the biometric, biomechanical, fibrillar and simulated IOP parameters between the BC subgroup and the other 6 subgroups. P values less than 0.05 were considered statistically significant.

3. Results

3.1. Central corneal thickness changes

As indicated in Figure 3, central corneal thickness (CCT) changes from pre to pos12w were significant ($p< 0.05$) in all 7 subgroups. In the 3 treated subgroups, CCT increased slightly with non-statistically significance from pre to pos2w ($p >0.05$), then decreased significantly from pos2w to pos12w ($p< 0.05$) to below the pre-treatment values (-21.6±21.5 μm in TRT, -12.3±22.7 μm in LAT, -14.9±19.4 μm in BIT). In contrast, the 4 control subgroups experienced continuous and significant increases in CCT between pre and pos12w stages (for TRC:10.7±12.7 μm, $p< 0.01$, for LAC: 11.9±13.8 μm, $p< 0.01$, for BIC: 10.1±10.2 μm, $p< 0.01$, for BC: 31.9±13.7 μm, $p< 0.01$). The CCT changes between pre and pos12w were also significantly different in TRT compared with TRC ($p< 0.01$), LAT compared with LAC ($p< 0.01$), and BIT compared with BIC ($p< 0.01$).

3.2. Intraocular pressure changes

As shown in Figure 4, IOP measured with the Tonopen decreased significantly from pre to pos2w in both eyes of rabbits treated with either travoprost, latanoprost or bimatoprost ($p< 0.05$) even though only one eye received treatment. The changes in IOP over the 12 week period were significant reductions in all 6 subgroups (all $p< 0.05$). The decreases in IOP at week 12 were similar ($p> 0.05$) among the 3 treated subgroups (-2.3±2.5 mmHg in TRT, -3.5±2.3 mmHg in LAT, -3.3±2.0 mmHg in BIT), and also ($p >0.05$) in the 3 control subgroups (-1.5±2.1 mmHg in TRC, -2.4±1.3 mmHg in TAC, -2.6±3.0 mmHg in BIC). The results also showed significant pos12w - pre IOP differences between the LAT and LAC subgroups ($p= 0.036$), but not between TRT and TRC subgroups ($p= 0.089$), or between BIT and BIC subgroups ($p= 0.288$). On the other hand, in the BC subgroup, the change in IOP from pre to pos12w was slight (0.1±1.8 mmHg) and insignificant ($p= 0.743$). These changes were significantly different when compared with all other 5 subgroups (all $p< 0.05$) except for TRC subgroup ($p =0.069$).

3.3 Inflation test results

As shown in Figure 5, a clear difference in pressure-apical displacement behaviour was

observed between the 2 treated subgroups and their corresponding control groups ($p < 0.05$) except for LAT and LAC ($p = 0.201$). The difference of apical displacement between 3 treated subgroups and the blank control subgroup were all statistically significant (all $p < 0.05$). It is also interesting to note that the control subgroups TRC, LAC and BIC – the fellow eyes of treated subgroups – experienced more displacement with non-statistically significance ($p > 0.05$), and hence showed lower mechanical stiffness, than the blank control group BC.

3.4 Inverse analysis results

Inverse analysis was used to derive a constitutive model for each cornea that provided the best possible match (lowest RMS) with the experimentally obtained pressure-displacement results. With the material parameters μ and α determined (Table 1), the stress-strain (σ-ε) relationships, and the tangent modulus ($Et = d\sigma/d\varepsilon$) at any stress level could be obtained. The mean stress-strain behavior for each subgroup is presented in Figure 6 and showed similar trends to those observed in the pressure-displacement behavior..

The stress-strain behavior allowed determination of Et at any stress level. Comparisons have been held at 3 stress levels of 2kPa, 4kPa and 6kPa that covered the initial nonlinear part of specimen behavior, Table 2. Compared with the BC subgroup, significant decreases in Et at 4kPa and 6kPa stress were found in the TRT subgroup ($p=0.007$ vs $p= 0.002$) but not in other subgroups (all $p> 0.05$). Significant differences in Et were also observed between TRT and TRC subgroup ($p= 0.026$ and $p= 0.022$ at 4kPa and 6kPa stresses), but not between LAT and LAC ($p= 0.583$ and $p= 0.538$), or between BIT and BIC ($p= 0.493$ and $p= 0.509$). The differences in Et between treated eyes and fellow control eyes were not statistically significant in all three treated groups at 2kPa stress stage (Table 3).

3.5 Histological Analysis

As indicated in Table 4, the mean fibril diameter was significantly smaller (all $p< 0.05$) at pos12w in both eyes of treated rabbits compared to the BC subgroup in the three stromal layers (anterior, intermediate and posterior). In contrast, the interfibrillar spacing showed the opposite trend, being significantly larger (all $p <0.05$) at pos12w in both eyes of treated rabbits compared

to the BC subgroup in the three stromal layers. The number of fibrils per unit area (μm^2) in the 3 treated rabbit groups (TRT, LAT, BIT) was not significantly different (all $p > 0.05$) from the BC subgroup. In contrast, the number of fibrils per unit area normalized by stromal thickness was significantly different in the TRT and LAT subgroups compared with the BC subgroup ($p < 0.05$) unlike the BIT subgroup ($p > 0.05$).

Bilaterally, differences in fibril diameter were significant between TRT and TRC subgroups in anterior stroma ($p = 0.013$), but otherwise were insignificant (all $p > 0.05$). For interfibrillar spacing and number of fibrils per unit area, all the differences between treated and corresponding control subgroups were not significant ($p > 0.05$) except for travoprost in intermediate stroma. As for the number of fibrils per unit area was normalized by stromal thickness, there was a reduction in the treated groups relative to their corresponding lateral control groups (all $p < 0.05$) except for LAT and BIT in medium stroma and LAT in anterior stroma ($p > 0.05$).

3.6 Finite element modelling of GAT IOP measurement process

The numerical simulations of the GAT applanation process led to the GAT-IOP estimations listed in Table 6. The results showed reductions in GAT estimations of IOP in all treated subgroups, compared to their corresponding control subgroups. The reductions in mean GAT-IOP values were -0.79±1.02, -1.57±1.93 and -2.36±2.85 mmHg in the travaprost group with IOP of 10, 20 and 30 mmHg, respectively (all $p < 0.05$). The corresponding reductions were -0.31±0.83, -0.57±1.45 and -0.86±2.14 mmHg in the latanoprost group (all $p > 0.05$) and -0.37±0.82, -0.67±1.58 and -0.99±2.29 mmHg in the bimatoprost group (all $p > 0.05$). Further, all GAT-IOP estimations in these six subgroups were lower than those in the BC subgroup with the differences being significant in all cases (all $p < 0.01$).

4. Discussion

Due to their outstanding IOP lowering potency and easy application (Al-Jazzaf et al., 2003), prostaglandin derivates (PGF2α) have become among the most widely used medicines in the

management of glaucoma - that is despite their well-documented side effects including conjunctival hyperemia (Stewart et al., 2003), ocular irritation (Day et al., 2006), iris pigmentation (Huang et al., 2009) and eyelid skin darkening (Yang et al., 2009). While the cytotoxicity of commercial PGF2α products have received much attention (Guenoun et al., 2005; Kahook and Ammar, 2010), few studies dealt with their influence on corneal biomechanics (Meda et al., 2017; Zheng et al., 2019). In an attempt to address this gap, this study used inflation testing and histological analysis and found significant differences in corneal material stiffness and stromal microstructure in rabbit eyes treated in-vivo with three kinds of PGF2α.

Earlier studies based on biomechanical measurements by the Ocular Response Analyzer (ORA) reported conflicting messages on the effect of PGF2α treatment on corneal biomechanics. The studies relied on the Corneal Hysteresis (CH) parameter – a measure of viscoelastic damping – and the Corneal Resistance Factor (CRF) – a measure of corneal stiffness. Both parameters were related to corneal biomechanics, although the links between them and standard biomechanical parameters such as the tangent modulus (Et) and tissue viscoelasticity were not established. An observational cross-sectional study found no changes in CH but decreases in CRF when comparing POAG patients receiving PGF2α treatment to those without the treatment (Detry-Morel et al., 2011), other studies compared CH and CRF before and during the follow-ups of the PGF2α treatment and found increases in CH after PGF2α treatment (Agarwal et al., 2012), increases in CH accompanied by no change in CRF (Tsikripis et al., 2013), increases in both CH and CRF (Liehneova and Karlovska, 2014), and decreases in both CH and CRF that were reversible following the cessation of the PGF2α treatment (Meda et al., 2017). a recent animal test using rabbits demonstrated no change in both CH and CRF after PGF2α treatment and no difference in both CH and CRF when comparing treated and untreated rabbit eyes (Lazcano-Gomez et al., 2016).

In a study employing the Corneal Visualization Scheimpflug Technology (Corvis ST, CVS), and after correcting for factors that potentially influence corneal dynamic parameters, a significant difference was detected in the deformation amplitude (DA) post PGF2α therapy (Wu

et al., 2016). This study, which was conducted before the Stress-Strain Index – intended to estimate the corneal material stiffness in vivo – became available in the Corvis ST software, relied on a parameter – the DA – whose strongest predictor was demonstrated to be IOP (Kling and Marcos, 2013) while its links to the standard biomechanical parameters were not clear. As a result, the effects of PGF2α on corneal biomechanical properties remained undecided.

In this study, inflation testing, considered superior to the much simpler strip extensometry testing (Elsheikh and Anderson, 2005; Hoeltzel et al., 1992), was used to quantify the tangent modulus of the tissue, measure of material stiffness. Keeping the cornea intact and at physiologic hydration on both the anterior and posterior surfaces, the test subjected the tissue to cycles of posterior pressure representing IOP and monitored the anterior surface's deformation through a combination of a laser beam and digital cameras. An inverse finite element analysis exercise was then used to estimate the stress-strain behavior and tangent modulus of corneal tissue. The changes in corneal material stiffness induced by in-vivo PGF2α usage were different among the three groups treated with travoprost, latanoprost and bimatoprost. Compared with the blank control group, the decreases in tangent modulus reduced from -38.3% in the TRT group, down to -26.9 % and -26.0 % in the LAT and BIT groups, respectively, at 6kPa stress. These decreases were significant ($p< 0.05$) in the TRT subgroup but not in the other groups. Interestingly, control corneas were stiffer than their lateral treated eyes, but softer than the blank control (BC) subgroup with no statistical significance (TRC: -18.2%; LAC: -20.6%; BIC: -19.2%).

A statistically significant reduction in CCT was observed earlier in patients with glaucoma or ocular hypertension submitted to monotherapy with prostaglandin analogues (travoprost 0.004%) (Schlote et al., 2009; Zhong et al., 2011). A similar significant reduction in corneal thickness (Schlote et al., 2009; Zhong et al., 2011) was observed in this study with PGF2α usage in all three treated subgroups compared with their three corresponding control subgroups. Further, all six subgroups maintained smaller CCT values relative to the blank control group (BC).

As for microstructure, corneal stroma contains abundant type I collagens secreted by keratocytes, and makes up the greatest part of corneal thickness (BenEzra and Foidart, 1981). Similar to Park's study, which showed a marked decrease in collagen type I in the PGF2α-treated group (Lopilly Park et al., 2012), the treated subgroups in our study, and their fellow untreated eyes, had significantly smaller fibril diameters compared with the BC group ($p< 0.05$). Meanwhile, the interfibrillar spacing of corneal stroma increased in two treated subgroups (37.00±3.90 nm in TRT and 32.26±3.82 nm in LAT) more than in the BC subgroup (20.42±1.12 nm). The spacing also became wider than in the blank control group while being narrower than their lateral treated eyes (32.12±3.23 nm in TRC and 34.79±4.52 nm in LAC) in the intermediate stromal layer. A similar trend was found in anterior and posterior stromal layers. Bilateral differences were only statistically significant between TRT and TRC for interfibrillar spacing.

Similar to our earlier study (Zheng et al., 2019), the histological results showed a significant increase in the collagen interfibrillar spacing in all three treated groups ($p< 0.05$), combined with a decrease in fibril diameter, indicating a decrease in collagen fiber density in corneal stroma. The changes were highest in the TRT group, followed by the LAT group and lowest in the BIT group. It was theorized that PGF2α could stimulate collagen gel contraction (Liu et al., 2006), decrease fibronectin proteins, cause degradation of collagen (Maruyama et al., 2014) and change collagen distribution in corneal stroma (Wu et al., 2005). Along with further effects in reducing stromal thickness (A. et al., 2003; Schrems et al., 2016; Zhong et al., 2011), the ultimate outcome could be weakening of corneal material stiffness. Different PGF2α's exhibited varying results in IOP reduction (Lin et al., 2014) and differential expression of MMPs in the ciliary body and ciliary muscle (Ooi et al., 2009; Yamada et al., 2016). Besides, different receptor subtypes of PGF2α's were proposed leading to different mechanisms to lower IOP (Ishida et al., 2006; Woodward et al., 1997). These differences may also result in variations in their effects on corneal microstructure and hence biomechanical properties.

The effect of PGF2α's in reducing corneal material stiffness may lead to underestimated IOP readings that can affect negatively the management of ocular diseases including glaucoma

(Huseynova et al., 2014). Compared with the blank control group, numerical simulations showed underestimations in GAT-IOP in the TRT subgroup between 15.1% and 17.0%, in LAT subgroup between 11.1% and 13.0 %, and in BIT subgroup between 11.9% and 13.9%. This notable effect raises an important question on the effectiveness of PGF2α's since part of the reductions in IOP readings could be an artifact caused by the effect of PGF2α's in reducing corneal stiffness. It is for this reason, that it is important to use new technology that provides biomechanically corrected IOP measurements.

PGF2α was shown to also affect the lateral eye, which did not undergo direct eyedrop treatment but this effect was smaller relative to that experienced by the treated eyes – this finding is similar to that reported by King (King and Rotchford, 2016; Rao et al., 2014). In our study, the loss in corneal material stiffness in the lateral eye led to GAT-IOP underestimations between 7.3% and 9.3% in the travoprost group, between 8.3% and 10.1% in the latanoprost group, and between 8.7% and 10.3% in the bimatoprost group. The systemic absorption of the medicine through the nasolacrimal mucosa and transport of the drug to the fellow eye via the blood stream might be the mechanism leading to the tissue softening observed in this study (Rao et al., 2014). This study is the first to report the influence of prostaglandin on the fellow eye, leading to changes in microstructure, reductions in tangent modulus and underestimations of IOP.

Rabbit eyes were used as an approximate model for the human eye in many experiments (Pellinen et al., 2012; Sjoquist et al., 1998), due to the difficulties in obtaining human donor eyes in sufficient numbers. However, due to differences between rabbit and human corneas (Hoeltzel et al., 1992; Jue and Maurice, 1986), and differences between ex-vivo and in-vivo measurements, the correlation between the findings of the present study and what to expect in human corneas and clinical usage should be approached with caution. Also, the finite element models used in the GAT simulation were limited in that average geometry and material parameters were assumed in all cases due to lack of specimen-specific measurements. However, an initial study on the effects of scleral settings on the final GAT readings demonstrated trivial variations in GAT readings with different scleral diameter and material parameters. The overall stiffness change of the sclera caused by changes in its geometry and material stiffness only had

significant effects on the peripheral cornea, while the central cornea, where the GAT tip applanates, was not affected. Therefore, the use of uniform scleral settings in all models should not invalidate the conclusions drawn herein.

The present study evaluated the changes in corneal biomechanical behavior caused by the application of three PGF2α's. The results demonstrated a significant corneal material stiffness reduction due to the use of PGF2α (especially travoprost, 0.004%), which warrant caution when clinicians assess adequacy of IOP control in patients under chronic PGF2α therapy. The study findings could help tailor the target IOP in clinical IOP-lowering treatment while considering the effect of PGF2α's on the IOP measurements made by GAT, the reference standard in tonometry.

References:

A., V., A., L., P., M., CY., M., 2003. Impact of prostaglandin F2-alpha agonists on the central corneal thickness. . Invest Ophth Vis Sci 44, U475-U475.

Agarwal, D.R., Ehrlich, J.R., Shimmyo, M., Radcliffe, N.M., 2012. The relationship between corneal hysteresis and the magnitude of intraocular pressure reduction with topical prostaglandin therapy. Br J Ophthalmol 96, 254-257.

Al-Jazzaf, A.M., DeSantis, L., Netland, P.A., 2003. Travoprost: a potent ocular hypotensive agent. Drugs Today (Barc) 39, 61-74.

Amano, S., Nakai, Y., Ko, A., Inoue, K., Wakakura, M., 2008. A case of keratoconus progression associated with the use of topical latanoprost. Jpn J Ophthalmol 52, 334-336.

Bao, F., Deng, M., Zheng, X., Li, L., Zhao, Y., Cao, S., Yu, A.Y., Wang, Q., Huang, J., Elsheikh, A., 2017. Effects of diabetes mellitus on biomechanical properties of the rabbit cornea. Exp Eye Res 161, 82-88.

Bao, F., Huang, Z., Huang, J., Wang, J., Deng, M., Li, L., Yu, A., Wang, Q., Elsheikh, A., 2016. Clinical Evaluation of Methods to Correct Intraocular Pressure Measurements by the Goldmann Applanation Tonometer, Ocular Response Analyzer, and Corvis ST Tonometer for the Effects of Corneal Stiffness Parameters. J Glaucoma 25, 510-519.

Bao, F., Wang, J., Cao, S., Liao, N., Shu, B., Zhao, Y., Li, Y., Zheng, X., Huang, J., Chen, S., Wang, Q., Elsheikh, A., 2018. Development and clinical verification of numerical simulation for laser in situ keratomileusis. J Mech Behav Biomed Mater 83, 126-134.

BenEzra, D., Foidart, J.M., 1981. Collagens and non collagenous proteins in the human eye. I. Corneal stroma in vivo and keratocyte production in vitro. Curr Eye Res 1, 101-110.

Day, D.G., Sharpe, E.D., Atkinson, M.J., Stewart, J.A., Stewart, W.C., 2006. The clinical validity of the treatment satisfaction survey for intraocular pressure in ocular hypertensive and glaucoma patients. Eye (Lond) 20, 583-590.

Detry-Morel, M., Jamart, J., Pourjavan, S., 2011. Evaluation of corneal biomechanical properties with the Reichert Ocular Response Analyzer. Eur J Ophthalmol 21, 138-148.

Dhaliwal, D.K., Romanowski, E.G., Yates, K.A., Hu, D., Mah, F.S., Fish, D.N., Gordon, Y.J., 2001. Valacyclovir inhibition of recovery of ocular herpes simplex virus type 1 after experimental reactivation by laser in situ

keratomileusis. J Cataract Refract Surg 27, 1288-1293.
Elsheikh, A., Anderson, K., 2005. Comparative study of corneal strip extensometry and inflation tests. J R Soc Interface 2, 177-185.
Elsheikh, A., Wang, D.F., Kotecha, A., Brown, M., Garway-Heath, D., 2006. Evaluation of goldmann applanation tonometry using a nonlinear finite element ocular model. Annals of Biomedical Engineering 34, 1628-1640.
Gabelt, B.T., Kaufman, P.L., 1989. Prostaglandin F2 alpha increases uveoscleral outflow in the cynomolgus monkey. Exp Eye Res 49, 389-402.
Grupcheva, C.N., Malik, T.Y., Craig, J.P., McGhee, C.N., 2001. In vivo confocal microscopy of corneal epithelial ingrowth through a laser in situ keratomileusis flap buttonhole. J Cataract Refract Surg 27, 1318-1322.
Guenoun, J.M., Baudouin, C., Rat, P., Pauly, A., Warnet, J.M., Brignole-Baudouin, F., 2005. In vitro comparison of cytoprotective and antioxidative effects of latanoprost, travoprost, and bimatoprost on conjunctiva-derived epithelial cells. Invest Ophthalmol Vis Sci 46, 4594-4599.
Hoeltzel, D.A., Altman, P., Buzard, K., Choe, K., 1992. Strip extensiometry for comparison of the mechanical response of bovine, rabbit, and human corneas. J Biomech Eng 114, 202-215.
Huang, P., Zhong, Z., Wu, L., Liu, W., 2009. Increased iridial pigmentation in Chinese eyes after use of travoprost 0.004%. J Glaucoma 18, 153-156.
Huseynova, T., Waring, G.O.t., Roberts, C., Krueger, R.R., Tomita, M., 2014. Corneal biomechanics as a function of intraocular pressure and pachymetry by Dynamic Infrared Signal and Scheimpflug Imaging Analysis in normal eyes. Am J Ophthalmol S0002-9394, 00814-00813.
Ishida, N., Odani-Kawabata, N., Shimazaki, A., Hara, H., 2006. Prostanoids in the therapy of glaucoma. Cardiovasc Drug Rev 24, 1-10.
Jonas, J.B., Aung, T., Bourne, R.R., Bron, A.M., Ritch, R., Panda-Jonas, S., 2017. Glaucoma. Lancet 390, 2183-2193.
Jue, B., Maurice, D.M., 1986. The mechanical properties of the rabbit and human cornea. J Biomech 19, 847-853.
Kahook, M.Y., Ammar, D.A., 2010. In vitro toxicity of topical ocular prostaglandin analogs and preservatives on corneal epithelial cells. J Ocul Pharmacol Ther 26, 259-263.
Kamiya, K., Aizawa, D., Igarashi, A., Komatsu, M., Shimizu, K., 2008. Effects of antiglaucoma drugs on refractive outcomes in eyes with myopic regression after laser in situ keratomileusis. Am J Ophthalmol 145, 233-238.
King, A.J., Rotchford, A.P., 2016. Validity of the Monocular Trial of Intraocular Pressure-Lowering at Different Time Points in Patients Starting Topical Glaucoma Medication. JAMA ophthalmology 134, 742-747.
Kling, S., Marcos, S., 2013. Contributing factors to corneal deformation in air puff measurements. Invest Ophthalmol Vis Sci 54, 5078-5085.
Lazcano-Gomez, G., Ancona-Lezama, D., Gil-Carrasco, F., Jimenez-Roman, J., 2016. Effects of topical travoprost 0.004% on intraocular pressure and corneal biomechanical properties in an animal model. Digital journal of ophthalmology : DJO / sponsored by Massachusetts Eye and Ear Infirmary 22, 1-5.
Lee, P.Y., Podos, S.M., Severin, C., 1984. Effect of prostaglandin F2 alpha on aqueous humor dynamics of rabbit, cat, and monkey. Invest Ophthalmol Vis Sci 25, 1087-1093.
Li, T., Lindsley, K., Rouse, B., Hong, H., Shi, Q., Friedman, D.S., Wormald, R., Dickersin, K., 2016. Comparative Effectiveness of First-Line Medications for Primary Open-Angle Glaucoma: A Systematic Review and Network Meta-analysis. Ophthalmology 123, 129-140.
Liehneova, I., Karlovska, S., 2014. [The glaucoma pharmacological treatment and biomechanical properties of the cornea]. Cesk Slov Oftalmol 70, 167-176.
Lin, L., Zhao, Y.J., Chew, P.T., Sng, C.C., Wong, H.T., Yip, L.W., Wu, T.S., Bautista, D., Teng, M., Khoo, A.L., Lim, B.P., 2014. Comparative efficacy and tolerability of topical prostaglandin analogues for primary open-angle glaucoma and ocular hypertension. Ann Pharmacother 48, 1585-1593.

Lindsey, J.D., Kashiwagi, K., Boyle, D., Kashiwagi, F., Firestein, G.S., Weinreb, R.N., 1996. Prostaglandins increase proMMP-1 and proMMP-3 secretion by human ciliary smooth muscle cells. Curr Eye Res 15, 869-875.
Liu, J., Roberts, C.J., 2005. Influence of corneal biomechanical properties on intraocular pressure measurement: quantitative analysis. J Cataract Refract Surg 31, 146-155.
Liu, Y., Yanai, R., Lu, Y., Hirano, S., Sagara, T., Nishida, T., 2006. Effects of antiglaucoma drugs on collagen gel contraction mediated by human corneal fibroblasts. J Glaucoma 15, 255-259.
Lopilly Park, H.Y., Kim, J.H., Lee, K.M., Park, C.K., 2012. Effect of prostaglandin analogues on tear proteomics and expression of cytokines and matrix metalloproteinases in the conjunctiva and cornea. Exp Eye Res 94, 13-21.
Maruyama, Y., Mori, K., Ikeda, Y., Ueno, M., Kinoshita, S., 2014. Effects of long-term topical prostaglandin therapy on central corneal thickness. J Ocul Pharmacol Ther 30, 440-444.
Mattson, M.S., Huynh, J., Wiseman, M., Coassin, M., Kornfield, J.A., Schwartz, D.M., 2010. An in vitro intact globe expansion method for evaluation of cross-linking treatments. Invest Ophthalmol Vis Sci 51, 3120-3128.
Meda, R., Wang, Q., Paoloni, D., Harasymowycz, P., Brunette, I., 2017. The impact of chronic use of prostaglandin analogues on the biomechanical properties of the cornea in patients with primary open-angle glaucoma. Br J Ophthalmol 101, 120-125.
Mulhern, M.G., Condon, P.I., O'Keefe, M., 2001. Myopic and hyperopic laser in situ keratomileusis retreatments: indications, techniques, limitations, and results. J Cataract Refract Surg 27, 1278-1287.
Ni, S., Yu, J., Bao, F., Li, J., Elsheikh, A., Wang, Q., 2011. Effect of glucose on the stress-strain behavior of ex-vivo rabbit cornea. Experimental eye research 92, 353-360.
Ooi, Y.H., Oh, D.J., Rhee, D.J., 2009. Effect of bimatoprost, latanoprost, and unoprostone on matrix metalloproteinases and their inhibitors in human ciliary body smooth muscle cells. Invest Ophthalmol Vis Sci 50, 5259-5265.
Pellinen, P., Huhtala, A., Tolonen, A., Lokkila, J., Maenpaa, J., Uusitalo, H., 2012. The cytotoxic effects of preserved and preservative-free prostaglandin analogs on human corneal and conjunctival epithelium in vitro and the distribution of benzalkonium chloride homologs in ocular surface tissues in vivo. Curr Eye Res 37, 145-154.
Rao, H.L., Senthil, S., Garudadri, C.S., 2014. Contralateral intraocular pressure lowering effect of prostaglandin analogues. Indian J Ophthalmol 62, 575-579.
Sagara, T., Gaton, D.D., Lindsey, J.D., Gabelt, B.T., Kaufman, P.L., Weinreb, R.N., 1999. Topical prostaglandin F2alpha treatment reduces collagen types I, III, and IV in the monkey uveoscleral outflow pathway. Arch Ophthalmol 117, 794-801.
Schachtschabel, U., Lindsey, J.D., Weinreb, R.N., 2000. The mechanism of action of prostaglandins on uveoscleral outflow. Curr Opin Ophthalmol 11, 112-115.
Schlote, T., Tzamalis, A., Kynigopoulos, M., 2009. Central corneal thickness during treatment with travoprost 0.004% in glaucoma patients. J Ocul Pharmacol Ther 25, 459-462.
Schrems, W.A., Schrems-Hoesl, L.M., Mardin, C.Y., Horn, F.K., Juenemann, A.G., Kruse, F.E., Braun, J.M., Laemmer, R., 2016. The Effect of Long-term Antiglaucomatous Drug Administration on Central Corneal Thickness. J Glaucoma 25, 274-280.
Sinha Roy, A., Dupps, W.J., Jr., 2011. Patient-specific computational modeling of keratoconus progression and differential responses to collagen cross-linking. Invest Ophthalmol Vis Sci 52, 9174-9187.
Sjoquist, B., Basu, S., Byding, P., Bergh, K., Stjernschantz, J., 1998. The pharmacokinetics of a new antiglaucoma drug, latanoprost, in the rabbit. Drug Metab Dispos 26, 745-754.
Stewart, W.C., Kolker, A.E., Stewart, J.A., Leech, J., Jackson, A.L., 2003. Conjunctival hyperemia in healthy subjects after short-term dosing with latanoprost, bimatoprost, and travoprost. Am J Ophthalmol 135, 314-320.
Tamm, E., Lutjen-Drecoll, E., Rohen, J.W., 1990. Age-related changes of the ciliary muscle in comparison with

changes induced by treatment with prostaglandin F2 alpha. An ultrastructural study in rhesus and cynomolgus monkeys. Mechanisms of ageing and development 51, 101-120.

Tsikripis, P., Papaconstantinou, D., Koutsandrea, C., Apostolopoulos, M., Georgalas, I., 2013. The effect of prostaglandin analogs on the biomechanical properties and central thickness of the cornea of patients with open-angle glaucoma: a 3-year study on 108 eyes. Drug design, development and therapy 7, 1149-1156.

Weinreb, R.N., Lindsey, J.D., Marchenko, G., Marchenko, N., Angert, M., Strongin, A., 2004. Prostaglandin FP agonists alter metalloproteinase gene expression in sclera. Invest Ophthalmol Vis Sci 45, 4368-4377.

Wollensak, G., Wilsch, M., Spoerl, E., Seiler, T., 2004. Collagen fiber diameter in the rabbit cornea after collagen crosslinking by riboflavin/UVA. Cornea 23, 503-507.

Woodward, D.F., Regan, J.W., Lake, S., Ocklind, A., 1997. The molecular biology and ocular distribution of prostanoid receptors. Surv Ophthalmol 41 Suppl 2, S15-21.

Wu, K.Y., Wang, H.Z., Hong, S.J., 2005. Effect of latanoprost on cultured porcine corneal stromal cells. Curr Eye Res 30, 871-879.

Wu, N., Chen, Y., Yu, X., Li, M., Wen, W., Sun, X., 2016. Changes in Corneal Biomechanical Properties after Long-Term Topical Prostaglandin Therapy. PLoS One 11, e0155527.

Xie, Y., Wang, M., Cong, Y., Cheng, M., Wang, S., Wang, G., 2018. The pilocarpine-induced ciliary body contraction affects the elastic modulus and collagen of cornea and sclera in early development. Biomed Pharmacother 108, 1816-1824.

Yamada, H., Yoneda, M., Gosho, M., Kato, T., Zako, M., 2016. Bimatoprost, latanoprost, and tafluprost induce differential expression of matrix metalloproteinases and tissue inhibitor of metalloproteinases. BMC Ophthalmol 16, 26.

Yang, H.K., Park, K.H., Kim, T.W., Kim, D.M., 2009. Deepening of eyelid superior sulcus during topical travoprost treatment. Jpn J Ophthalmol 53, 176-179.

Yu, J.G., Bao, F.J., Feng, Y.F., Whitford, C., Ye, T., Huang, Y.B., Wang, Q.M., Elsheikh, A., 2013. Assessment of corneal biomechanical behavior under posterior and anterior pressure. J Refract Surg 29, 64-70.

Yu, J.G., Bao, F.J., Joda, A., Fu, X.A., Zhou, S., Wang, J., Hu, X.L., Wang, Q.M., Elsheikh, A., 2014. Influence of glucocorticosteroids on the biomechanical properties of in-vivo rabbit cornea. J Mech Behav Biomed Mater 29, 350-359.

Zhang, R., Xie, R., Zhou, X., Lv, F., Qu, J., 2015. Comparison of normal corneal structures with light microscope and electron microscope in seven animals. Ophthalmol CHN 24, 341-347.

Zheng, X., Bao, F., Geraghty, B., Huang, J., Yu, A., Wang, Q., 2016. High intercorneal symmetry in corneal biomechanical metrics. Eye and vision 3, 7.

Zheng, X., Wang, Y., Zhao, Y., Cao, S., Zhu, R., Huang, W., Yu, A., Huang, J., Wang, Q., Wang, J., Bao, F., Elsheikh, A., 2019. Experimental Evaluation of Travoprost-Induced Changes in Biomechanical Behavior of Ex-Vivo Rabbit Corneas. Curr Eye Res 44, 19-24.

Zhong, Y., Shen, X., Yu, J., Tan, H., Cheng, Y., 2011. The comparison of the effects of latanoprost, travoprost, and bimatoprost on central corneal thickness. Cornea 30, 861-864.

Zhu, R., Zheng, X., Guo, L., Zhao, Y., Wang, Y., Wu, J., Yu, A., Wang, J., Bao, F., Elsheikh, A., 2020. Biomechanical Effects of Two Forms of PGF2α on Ex-vivo Rabbit Cornea. Curr Eye Res, 1-9.

Figure Captions

Figure 1 Corneal profile (A) captured before the start of the inflation test by one of the three cameras mounted on the inflation rig (B) and used to construct specimen-specific numerical models (C)

Figure 2 Corneal applanation is achieved fully when the distance between the GAT tip edge and the corneal surface equals to the tear film thickness (adopted as 15 μm in the current study)

Figure 3 Changes in CCT during a 12-week follow-up period in the seven subgroups

Figure 4 Changes in IOP over the 12-week follow-up period in all subgroups

Figure 5 Mean pressure-displacement behavior at the corneal apex in all subgroups

Figure 6 Mean stress-strain behavior of corneas in all subgroups – error bars represent standard deviation of stress values

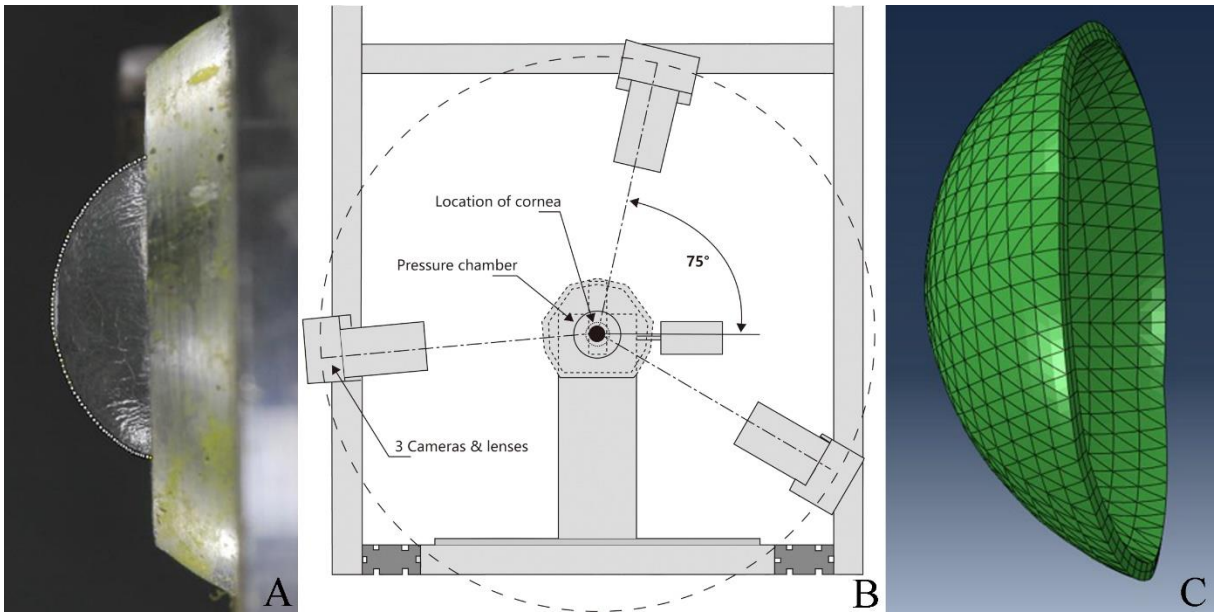

Figure 1 Corneal profile (A) captured before the start of the inflation test by one of the three cameras mounted on the inflation rig (B) and used to construct specimen-specific numerical models (C)

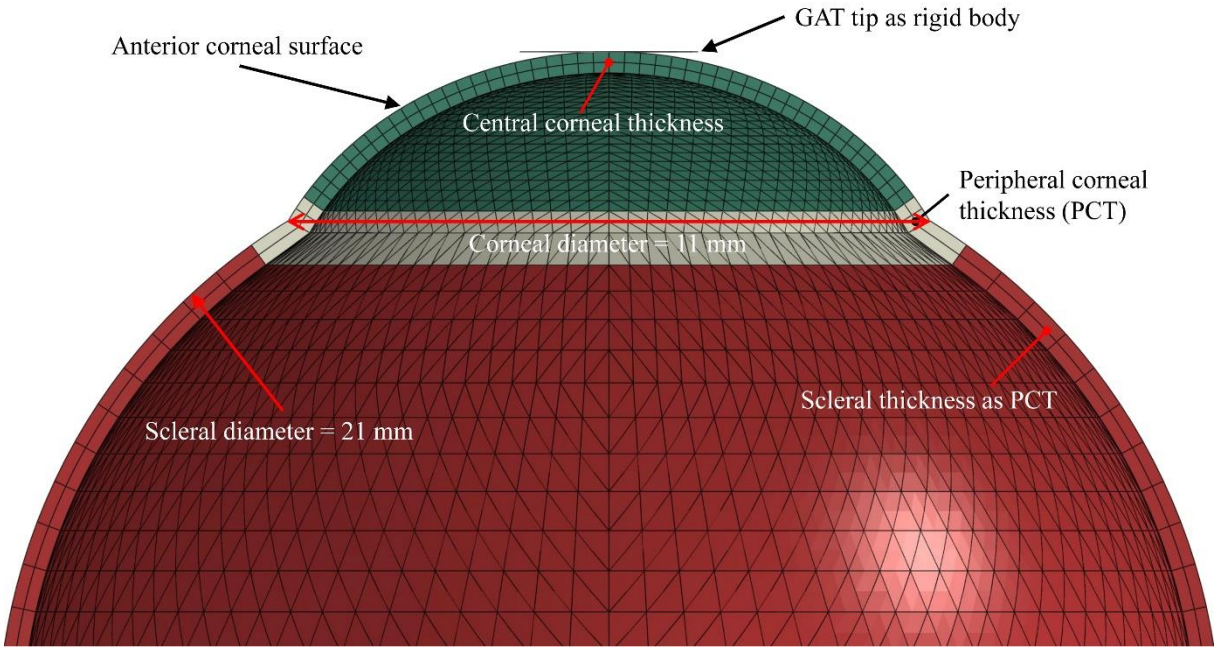

Figure 2 Corneal applanation is achieved fully when the distance between the GAT tip edge and the corneal surface equals to the tear film thickness (adopted as 15 μm in the current study), limbus adopt the same material settings as the sclera

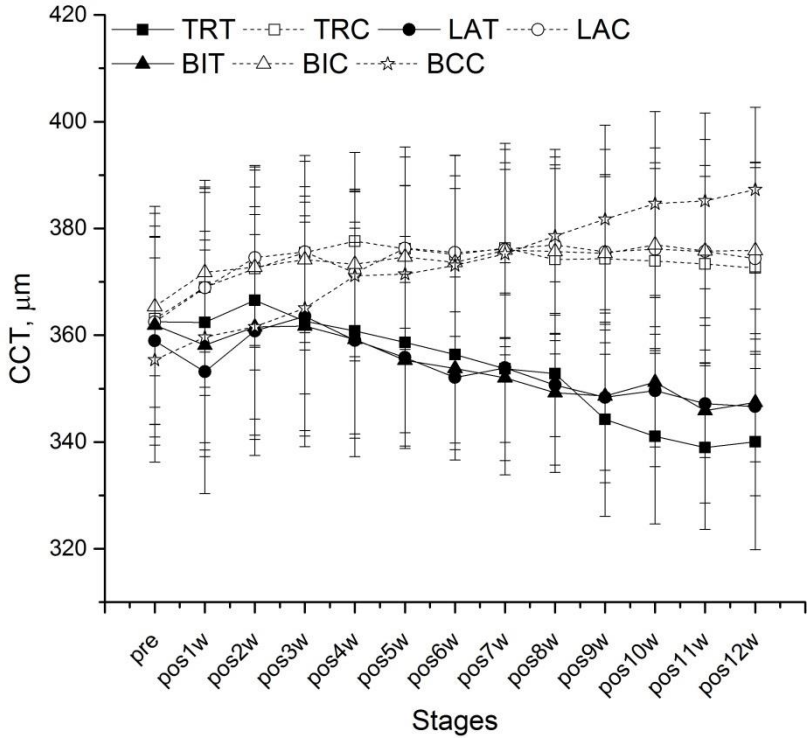

Figure 3 Changes in CCT during a 12-week follow-up period in the seven subgroups. Left eyes treated with travoprost, latanoprost and bimatoprost formed the TRT, LAT and BIT subgroups, while the fellow eyes were untreated and formed the TRC, LAC and BIC subgroups. The left eyes in the blank control group was named the BC subgroup

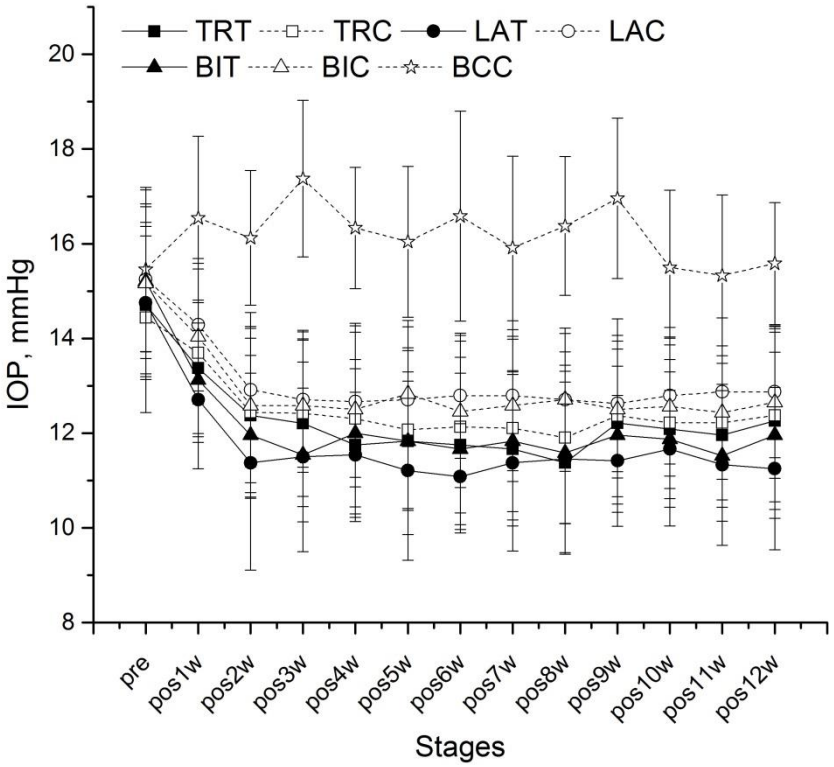

Figure 4 Changes in IOP over the 12-week follow-up period in all subgroups. Left eyes treated with travoprost, latanoprost and bimatoprost formed the TRT, LAT and BIT subgroups, while the fellow eyes formed the control subgroups TRC, LAC and BIC. The left eyes in the blank control group were named the BC subgroup

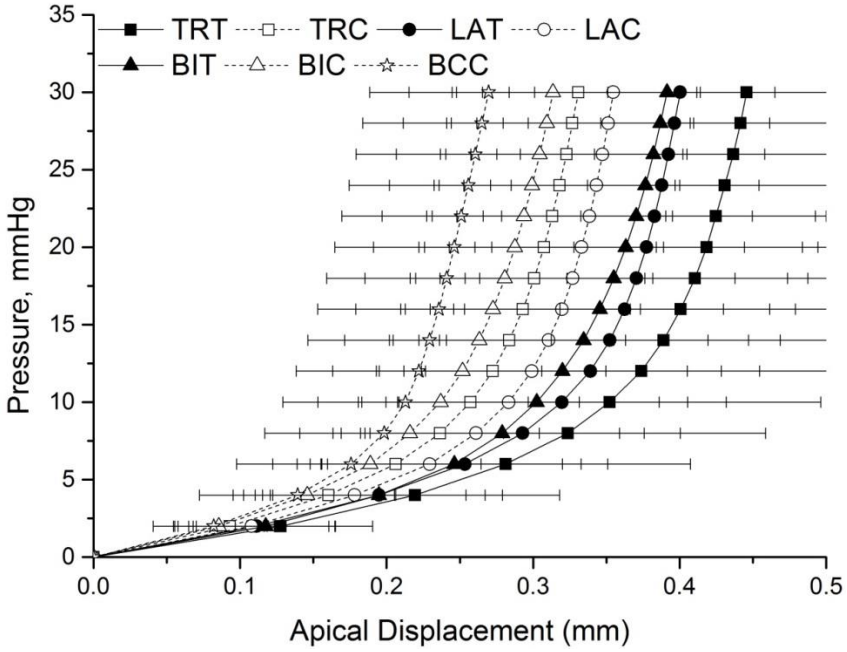

Figure 5 Mean pressure-displacement behavior at the corneal apex in all subgroups

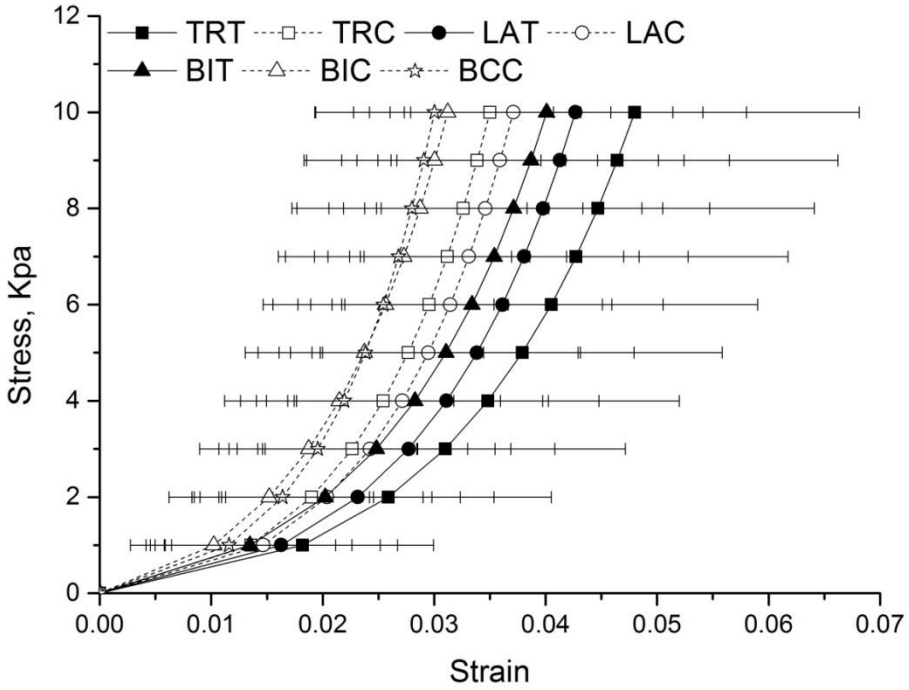

Figure 6 Mean stress-strain behavior of corneas in all subgroups – error bars represent standard deviation of stress values

Table Captions

Table 1 Mean and standard deviation of constitutive parameters μ and α in all subgroups

Table 2 Mean and standard deviation of tangent modulus in all subgroups at different stress levels

Table 3 Significance (p value) of differences in the Et values calculated at 2 kPa (top line), 4 kPa (middle line) and 6 kPa (bottom line)

Table 4 Mean and standard deviation of interfibrillar spacing and fibril diameter in corneal stroma in all subgroups

Table 5 Significance (p value) of differences in number of fibrils normalized by stromal thickness in anterior stroma (top line), medium stroma (middle line) and posterior stroma (bottom line)

Table 6 Mean and standard deviation of GAT-IOP measurements in all subgroups

Table 1 Mean and standard deviation of constitutive parameters μ and α in all subgroups

Group	μ, MPa	α	RMS, mm
TRT	0.0251±0.0305	74.57±25.34	0.0014±0.0014
TRC	0.0295±0.0257	96.12±23.37	0.0013±0.0013
LAT	0.0243±0.0245	84.16±21.26	0.0013±0.0012
LAC	0.0312±0.0321	95.84±25.83	0.001±0.0009
BIT	0.0290±0.0280	84.72±28.81	0.0009±0.0009
BIC	0.0400±0.0307	95.14±29.41	0.0008±0.0011
BC	0.0342±0.0353	121.18±39.86	0.0027±0.0033

Table 2 Mean and standard deviation of tangent modulus in all subgroups at different stress levels

Group	Et at different stress levels, MPa		
	2 kPa	4 kPa	6 kPa
TRT	0.19±0.08	0.32±0.11	0.46±0.15
TRC	0.24±0.06	0.42±0.10	0.61±0.15
LAT	0.23±0.16	0.38±0.21	0.54±0.26
LAC	0.24±0.08	0.42±0.10	0.59±0.15
BIT	0.23±0.17	0.39±0.22	0.55±0.29
BIC	0.26±0.09	0.43±0.12	0.60±0.17
BC	0.30±0.11	0.52±0.16	0.74±0.23

Table 3 Significance (p value) of differences in the Et values calculated at 2 kPa (top line), 4 kPa (middle line) and 6 kPa (bottom line)

	TRT	TRC	LAT	LAC	BIT	BIC	BC
		0.073	1.000	1.000	1.000	1.000	0.152
TRT	-	0.026*	1.000	1.000	1.000	1.000	0.007**
		0.022*	1.000	1.000	1.000	0.966	0.002**
			1.000	1.000	1.000	1.000	1.000
TRC	-	-	1.000	1.000	1.000	1.000	1.000
			1.000	1.000	1.000	1.000	1.000
				0.692	1.000	1.000	1.000
LAT	-	-	-	0.583	1.000	1.000	0.237
				0.538	1.000	1.000	0.115
					1.000	1.000	1.000
LAC	-	-	-	-	1.000	1.000	1.000
					1.000	1.000	0.681
						0.483	1.000
BIT	-	-	-	-	-	0.493	0.330
						0.509	0.154
							1.000
BIC	-	-	-	-	-	-	1.000
							0.970

* $p<0.05$, ** $p<0.01$

Table 4 Mean and standard deviation of interfibrillar spacing and fibril diameter in corneal stroma in all subgroups

	Group	n	Fibril diameter (nm)	Interfibrillar spacing (nm)	Number of fibrils per unit area	Number of fibrils normalized by stromal thickness
Anterior Stroma	TRT	6	21.51±0.75	34.36±4.38	420.13±61.44	121074.93±13074.89
	TRC	6	21.60±0.99	29.91±5.11	481.48±82.92	159430.82±23175.15
	LAT	6	21.61±1.13	33.91±1.18	414.35±29.34	119883.25±6235.81
	LAC	6	22.09±0.95	32.32±2.56	433.79±53.65	142914.92±18559.77
	BIT	6	21.22±0.49	29.62±3.66	498.11±67.89	143962.11±16753.19
	BIC	6	21.52±0.83	29.23±4.67	506.21±103.35	165510.42±24878.72
	BC	6	31.12±1.71	19.23±1.43	506.58±58.44	178294.84±19619.51
Medium Stroma	TRT	6	22.36±2.08	37.00±3.90	373.18±70.56	107610.16±17585.08
	TRC	6	21.71±1.03	32.12±3.23	432.95±60.27	143695.10±18140.62
	LAT	6	21.26±1.15	32.26±3.82	451.05±71.25	130268.69±17505.17
	LAC	6	21.83±1.13	31.47±2.81	455.23±47.34	149903.01±15956.57
	BIT	6	20.98±1.07	30.41±2.86	486.35±57.36	140821.32±16137.51
	BIC	6	21.36±0.71	28.70±4.74	519.36±97.24	170253.00±26234.26
	BC	6	31.72±1.64	20.42±1.12	471.16±46.99	165750.71±14818.40
Posterior Stroma	TRT	6	22.06±0.92	33.54±3.72	424.27±57.39	122569.05±14252.06
	TRC	6	21.15±0.75	30.42±3.81	477.57±70.23	158436.07±20885.00
	LAT	6	22.11±1.99	33.78±4.09	413.64±63.19	119971.50±19715.07
	LAC	6	22.32±1.23	32.54±2.29	424.79±34.92	139826.45±11041.24
	BIT	6	22.15±1.23	30.85±4.16	461.77±69.51	133609.03±18816.83
	BIC	6	21.81±1.00	28.62±5.02	506.75±95.25	165972.86±25697.87
	BC	6	30.89±1.86	21.35±1.78	472.30±67.76	166096.19±21878.92

Table 5 Significance (p value) of differences in number of fibrils normalized by stromal thickness in anterior stroma (top line), medium stroma (middle line) and posterior stroma (bottom line)

	TRT	TRC	LAT	LAC	BIT	BIC	BC
		0.019*	1.000	0.999	0.806	0.004**	0.000**
TRT	-	0.001**	0.839	0.007**	0.074	0.000**	0.000**
		0.007**	1.000	1.000	1.000	0.010**	0.009**
			0.015*	1.000	1.000	1.000	1.000
TRC	-	-	1.000	1.000	1.000	0.361	0.949
			0.033	1.000	0.704	1.000	1.000
				0.054	0.628	0.003**	0.000**
LAT	-	-	-	0.113	1.000	0.013*	0.042*
				0.018*	1.000	0.005**	0.005**
					1.000	0.856	0.044*
LAC	-	-	-	-	1.000	1.000	1.000
					1.000	0.539	0.525
						0.006**	0.057
BIT	-	-	-	-	-	0.068	1.000
						0.028*	0.136
							1.000
BIC	-	-	-	-	-	-	1.000
							1.000

* $p<0.05$, ** $p<0.01$

Table 6 Mean and standard deviation of GAT-IOP measurements in all subgroups

Group	n	IOP estimations		
		True IOP = 10 mmHg	True IOP = 20 mmHg	True IOP = 30 mmHg
TRT	18	8.58±0.78	17.23±1.50	25.78±2.22
TRC	18	9.37±0.54	18.79±1.05	28.14±1.57
LAT	18	8.99±0.83	18.04±1.38	27.00±2.04
LAC	18	9.30±0.60	18.61±1.13	27.86±1.66
BIT	18	8.90±0.78	17.85±1.44	26.75±2.08
BIC	18	9.27±0.64	18.52±1.24	27.74±1.82
BC	18	10.34±1.17	20.44±1.67	30.37±2.15